Available online at www.sciencedirect.com

SciVerse ScienceDirect

Journal of Nutritional Biochemistry 23 (2012) 76–84

Journal of Nutritional Biochemistry

Kuguacin J isolated from *Momordica charantia* leaves inhibits P-glycoprotein (ABCB1)-mediated multidrug resistance

Pornsiri Pitchakarn[a], Shinobu Ohnuma[b], Komsak Pintha[a], Wilart Pompimon[c], Suresh V. Ambudkar[b], Pornngarm Limtrakul[a,*]

[a]*Department of Biochemistry, Faculty of Medicine, Chiang Mai University, Chiang Mai 50200, Thailand*
[b]*Laboratory of Cell Biology, Center for Cancer Research, National Cancer Institute, National Institutes of Health, Bethesda, MD 20892, USA*
[c]*Laboratory of Natural Products, Department of Chemistry, Faculty of Science, Lampang Rajabhat University, Lampang 52100, Thailand*

Received 23 March 2010; received in revised form 22 October 2010; accepted 3 November 2010

Abstract

Multidrug resistance (MDR) is a major factor in the failure of chemotherapy in cancer patients. Resistance to chemotherapy has been correlated to the overexpression of ABC drug transporters including P-glycoprotein (P-gp) that actively efflux chemotherapeutic drugs from cancer cells. Our previous study showed that bitter melon (*Momordica charantia*) leaf extract (BMLE) was able to reverse the MDR phenotype by increasing the intracellular accumulation of chemotherapeutic drugs. In the present study, bioguided fractionation was used to identify the active component(s) of BMLE that is able to modulate the function of P-gp and the MDR phenotype in a human cervical carcinoma cell line (KB-V1). We found that kuguacin J, one of the active components in BMLE, increased sensitivity to vinblastine and paclitaxel in KB-V1 cells. A flow cytometry assay indicated that kuguacin J inhibits the transport function of P-gp and thereby significantly increases the accumulation of rhodamine 123 and calcein AM in the cells. These results were confirmed by [^{3}H]-vinblastine transport assay. Kuguacin J significantly increases intracellular [^{3}H]-vinblastine accumulation and decreased the [^{3}H]-vinblastine efflux in the cells. Kuguacin J also inhibited the incorporation of [^{125}I]-iodoarylazidoprazosin into P-gp in a concentration-dependent manner, indicating that kuguacin J directly interacts with the drug-substrate-binding site on P-gp. These results indicate that kuguacin J modulates the function of P-gp by directly interacting at the drug-substrate-binding site, and it appears to be an effective inhibitor of P-gp activity in vitro and thus could be developed as an effective chemosensitizer to treat multidrug-resistant cancers.

Keywords: ABC transporter; Bitter melon; Chemosensitivity; Multidrug resistance; P-glycoprotein; Kuguacin J

1. Introduction

Drug resistance is a major impediment to the treatment of cancer patients receiving single or multiple drugs. Efforts to reverse the drug resistance of tumor cells have been largely unsuccessful [1]. In recent years, considerable research has been directed toward understanding the underlying mechanisms that confer drug resistance. One major cause of drug resistance is the overexpression of the 170-kDa plasma membrane P-glycoprotein (P-gp). P-glycoprotein is a member of the highly conserved superfamily of ATP-binding cassette (ABC) transporter proteins. It acts as an ATP-driven efflux pump that decreases intracellular drug accumulation, thereby decreasing the effectiveness of many chemotherapeutic agents [2–5]. Several classes of synthetic compounds that inhibit P-gp-mediated efflux and enhance the accumulation and efficacy of anticancer agents have been identified. However, the efficacy of these compounds in animal studies and clinical trials has been disappointing due to dose-limiting toxicity [6]. Multidrug resistance (MDR)-reversing agents from natural products or plant-derived chemicals which have no toxicological effects are being investigated.

Momordica charantia L. or bitter melon is widely consumed as a vegetable and especially as a folk medicine in Asia. Extracts of bitter melon have been reported to possess antitumor activity such as inhibition of mouse spontaneous mammary tumorigenesis [7] and benzo(a)pyrene-induced mouse forestomach tumorigenesis [8]. Moreover, antioxidant activities [9] and antiviral [10], anti-diabetic and immunomodulating properties [11] of this plant also have been explored.

Our previous study demonstrated that bitter melon leaf extract (BMLE) reversed the MDR phenotype, increased the intracellular accumulation of [^{3}H]-vinblastine, decreased the [^{3}H]-vinblastine efflux in KB-V1 cells and increased their sensitivity to vinblastine [12]. In this study, bioguided fractionation was used to identify the active component(s) of BMLE that modulates the function of P-gp and the MDR phenotype in multidrug-resistant human cervical carcinoma KB-V1 cells. Our results revealed that kuguacin J, a known triterpenoid from BMLE, inhibits P-gp-mediated drug efflux, leading to an increase of the intracellular accumulation and cytotoxicity of

* Corresponding author. Tel.: +66 53 945325 6x218; fax: +66 53 217144 or 894031.
E-mail address: plimtrak@med.cmu.ac.th (P. Limtrakul).

0955-2863/$ - see front matter © 2012 Elsevier Inc. All rights reserved.
doi:10.1016/j.jnutbio.2010.11.005

chemotherapeutic drugs in drug-resistant human cervical carcinoma cells in vitro.

2. Materials and methods

2.1. Chemicals

[^{3}H]-Vinblastine (10.8 Ci/mmol) was obtained from Amersham Bioscience (Cardiff, UK). Cyclosporin A (CsA), verapamil (Ver), vinblastine (Vin), paclitaxel (Pacl) and 3-(4,5 dimethylthiazol-2-yl)-2,5-diphenyltetrazolium bromide (MTT) were obtained from Sigma Chemical Company (St. Louis, MO, USA). Dulbecco's modified Eagle's medium (DMEM) was purchased from Gibco BRL (Grand Island, NY, USA). Calcein-AM (C-AM) and Rhodamine123 (Rh123) were obtained from Molecular Probes, Inc. (Eugene, OR, USA). [^{125}I]Iodoarylazidoprazosin (IAAP) was purchased from Perkin Elmer Life Science (Wellesley, MA, USA).

2.2. Preparation and isolation of bitter melon extracts

Leaves of bitter melon were collected in Lampang province, Thailand. A voucher specimen (BKF no. 15602) has been deposited at the Forest Herbarium, Department of National Park, Wildlife and Plant Conservation, Ministry of Natural Resources and Environment, Bangkok, Thailand. The fresh leaves were dried at 30°C–45°C and ground. Dried powdery plant samples (1 kg) were extracted exhaustively with 4 L of 80% ethanol by maceration at 37°C for 16 h. The mixture was filtered and reextracted with 4 L of ethanol. The combined filtrate was bleached with 160 g of active charcoal, filtered and concentrated by rotary evaporation to 120 ml before filtering to remove precipitates. The filtrate was rotary evaporated and lyophilized. One hundred grams of residue was redissolved in 1 L of 50% methanol and successively partitioned with hexane, diethyl ether, chloroform, ethyl acetate and an aqueous layer. Each fraction was dried under reduced pressure and then submitted for bioassays. From the bioassay-guided fractionation, the diethyl ether fraction was separated by column chromatography. The diethyl ether extract (15 g) was separated by column chromatography over silica gel (Merck, 70-230 mesh ASTM, cat. no. 7734) 100 g, eluting with various proportions of ethyl acetate-n-hexane, followed by the increasing volume of methanol in ethyl acetate and finally with pure methanol. Fractions (50 ml each) were collected and combined on the basis of TLC behavior. The solvents were evaporated to dryness to afford eight fractions (F_1–F_8). Fraction F_2 (2.85 g), which eluted by 30% ethyl acetate-n-hexane, was obtained as white solids mixed with fat. Further separation by column chromatography over silica gel 50 g was performed. Gradient elution was started from pure n-hexane, gradually enriched with ethyl acetate in hexane up to 20% methanol–ethyl acetate. Fractions were collected and combined, and then solvent was removed under reduced pressure to afford subfraction A_1. Further, the subfraction A_1 (1.89 g) was separated by column chromatography over silica gel to yield white crystals of subfraction B1 (1.23 g). The crystals were recrystallized with 95% ethanol to give purified white crystals 1.10 g, which were identified as kuguacin J (Fig. 2A).

2.3. Cells and cell culture

An MDR cervical carcinoma cell line (KB-V1) and a drug-sensitive cervical carcinoma cell line (KB-3-1) were generous gifts from Dr. Michael M. Gottesman (National Cancer Institute, Bethesda, MD, USA). Both cell lines were cultured in DMEM with 4.5 g of glucose/L plus 10% fetal bovine serum, 5 mM l-glutamine, 50 U/ml penicillin and 50 g/ml streptomycin; 1 g/ml of vinblastine was added only to the KB-V1 culture medium. These two cell lines were maintained in a humidified incubator with an atmosphere comprising 95% air and 5% CO_2 at 37°C. When the cells reached 70%–80% confluence, they were harvested and plated either for subsequent passages or for drug treatments.

2.4. Measurement of paclitaxel and vinblastine cytotoxicity

KB-V1 and KB-3-1 cells were plated at 2.0×10^3 cells per well in 96-well plates. After 24 h, BMLE or kuguacin J and various concentrations of vinblastine or paclitaxel were added. The cells were incubated for 48 h at 37°C, and then cell growth was assessed by means of an MTT colorimetric assay [12]. In each experiment, determinations were carried out in triplicate. Relative resistance was calculated as the ratio of the IC_{50} value of the KB-V1 cells to the IC_{50} value of the KB-3-1 cells.

2.5. Accumulation of fluorescent substrates

To measure accumulation of Rh123 [2], KB-V1 and KB-3-1 cells (5×10^5) were incubated with 200 ng/ml of Rh123 for 30 min at 37°C in DMEM without phenol red medium either with or without MDR1 modulators (5 μM CsA or 20 μM Ver or various concentrations of kuguacin J). The cells were washed twice with ice-cold phosphate-buffered saline (PBS) and resuspended in 0.1% bovine serum albumin (BSA)–PBS. Samples were analyzed on a FACScan flow cytometer (Becton Dickinson, San Jose, CA, USA) equipped with a 488-nm argon laser. The green fluorescence of Rh123 was measured by a 530 nm band-pass filter (hLi). To measure accumulation of C-AM [13], KB-V1 and KB-3-1 cells (5×10^5) were incubated with 0.1 μmol/L of C-AM for 15 min at 37°C in DMEM without phenol red medium either with or without the MDR1 modulators (5 μM CsA or 20 μM Ver or various concentrations of kuguacin J). The cells were washed twice with ice-cold PBS and resuspended in 0.1% BSA–PBS. Samples were immediately analyzed on a FACScan flow cytometer.

2.6. Radiolabeled drug transportation

The effect of BMLE on P-gp-mediated drug transport was confirmed by monitoring the intracellular radiolabeled drug accumulation using a [^{3}H]-vinblastine incorporation assay [12]. The cells (6.0×10^5 cells/well) were cultured in complete DMEM for 24 h, and then the cells were treated with various concentrations of BMLE or kuguacin J or the MDR-reversing agent (10 μM CSA or 20 μM Ver) in the presence of 0.05 μCi [^{3}H]-vinblastine/ml for 60 min. After washing with ice-cold PBS (pH 7.4), the cells were harvested, and then the amount of intracellular radioactivity was measured.

To determine the drug efflux [14], the cells were seeded as described above in the drug accumulation experiments. Cells were incubated for 60 min at 37°C with 0.05 μCi [^{3}H]-vinblastine/ml in the presence of 20 μM Ver in order to load the cells with radiolabeled drug. The cells were then washed with ice-cold PBS (pH 7.4) and then treated with various concentrations of BMLE or kuguacin J or the reversing agent (10 μM CSA or 20 μM Ver). After incubation at 37°C for 30 min, cells were washed with ice-cold PBS (pH 7.4), and the amount of intracellular radioactivity was measured as described above.

2.7. Preparation of crude membranes from P-gp-expressing High Five insect cells

High Five insect cells (Invitrogen, Carlsbad, CA, USA) were infected with the recombinant baculovirus carrying the human *MDR*1 cDNA with a 6× Histidine tag at the C-terminal end as described [15]. Crude membranes were prepared as described previously [16].

2.8. Photoaffinity labeling with [^{125}I]-IAAP

The crude membranes of P-gp-expressing High Five insect cells (60 μg) were incubated with varying concentrations of kuguacin J (0–50 μM) in 100 μl of 50 mM Tris–HCl, pH 7.5, at room temperature for 5 min. Then, 4–6 nM [^{125}I]-IAAP (2200 Ci/mmol) was added and incubated for 5 min under subdued light. The samples were photo-crosslinked with a UV lamp (365 nm) for 5 min at room temperature, and 20 μg of each sample was electrophoresed on a 7% Tris–acetate gel. The gel was dried and exposed to X-ray film for 3–6 h at -80°C. The signals of [^{125}I]-IAAP incorporated into P-gp were quantified using the STORM 860 phosphor imager system (Molecular Dynamics, Sunnyvale, CA, USA) and the software ImageQuant TL (GE Healthcare, Piscataway, NJ, USA) [16].

2.9. ATPase assay

Crude membrane protein (10 μg) from High Five cells expressing P-gp were incubated at room temperature for 5 min with varying concentrations of kuguacin J (0–25 μM) in the presence and absence of sodium orthovanadate (Vi) (0.3 mM) in 100 μl of ATPase assay buffer (50 mM Mes–Tris, pH 6.8, 50 mM KCl, 5 mM sodium azido, 10 mM $MgCl_2$, 2 mM DTT, 1 mM EGTA, 1 mM ouabain). The reaction was initiated by the addition of 5 mM ATP and incubated for 20 min at 37°C. Sodium dodecyl sulfate (SDS) solution (0.1 ml of 5% SDS) was added to terminate the reaction, and the amount of inorganic phosphate released was quantified with a colorimetric reaction, as described previously [17]. The specific activity was recorded as Vi-sensitive ATPase activity.

2.10. Statistical analysis

The results are presented as means±S.D. from triplicate samples of three independent experiments. Differences between the means were analyzed by one-way analysis of variance and Student's *t* test. Statistical significance was considered when $P<.05$ or $P<.01$. All statistical analyses were performed using SPSS 10.0 software.

3. Results

3.1. P-glycoprotein (ABCB1)-mediated MDR-reversing properties of BMLE and bioguided fractionation

In order to isolate the compound(s) responsible for P-gp reversing properties, a bioguided fractionation strategy was performed throughout the separation procedure (see preparation and isolation in Materials and methods). We examined the modulation of the MDR phenotype of the total ethanol extract and the hexane, diethyl ether, chloroform, ethyl acetate and residue fractions combined with vinblastine. The results showed that the hexane and diethyl ether fractions (50 μg/ml; noncytotoxic concentration) had the highest

Table 1
Modulation of resistance to vinblastine in KB cells by total ethanol, hexane and diethyl ether fractions from bitter melon leaves

	IC_{50}[a]	Relative resistance[b]
Vinblastine treatment		
KB-3-1	0.7±0.04 nM	1
KB-V1	1.5±0.07 μM	2143
Total ethanol extract		
KB-V1+2.5 μg/ml of the extract	1.2±0.28 μM	1714
KB-V1+5 μg/ml of the extract	0.9±0.35 μM	1286
Hexane fraction		
KB-V1+2.5 μg/ml of the extract	0.9±0.14 μM	1286
KB-V1+5 μg/ml of the extract	0.5±0.11 μM	714*
Diethyl ether fraction		
KB-V1+2.5 μg/ml of the extract	0.8±0.19 μM	1142
KB-V1+5 μg/ml of the extract	0.6±0.05 μM	857*

*P<.05; **P<.01, vs. control treated without hexane and diethyl ether fractions.
[a] Determined by the MTT assay, and the values are means±S.D. of three independent experiments.
[b] IC_{50} of KB-V1/IC50 of KB-3-1. Each point represents the mean (±S.D.) of three independent experiments performed in triplicate.

MDR-reversing properties and decreased the IC_{50} of vinblastine in KB-V1 cells in a dose-dependent manner, while similar treatment of KB-3-1 cells showed no modulating effect. The MDR-reversing properties of the total ethanol extract and the hexane and diethyl ether fractions are shown in Table 1. Moreover, these fractions were tested by [^{3}H]-vinblastine incorporation assay. The results indicated that the hexane and diethyl ether fractions increased intracellular [^{3}H]-vinblastine accumulation and decreased the [^{3}H]-vinblastine efflux in KB-V1 cells in a concentration-dependent manner, while no change was observed in KB-3-1 cells (Fig. 1).

As the percentage yield of diethyl ether fraction was higher than hexane fraction, we therefore purified the active ingredient(s) which plays important roles in P-gp modulation using the diethyl ether fraction as a staring material (Materials and methods). Eight fractions were collected, and it was found that fraction F_2 provided the highest MDR-reversing property (data not shown). The fraction F_2 was further separated according to Materials and methods and yielded subfraction B1, a purified white crystal.

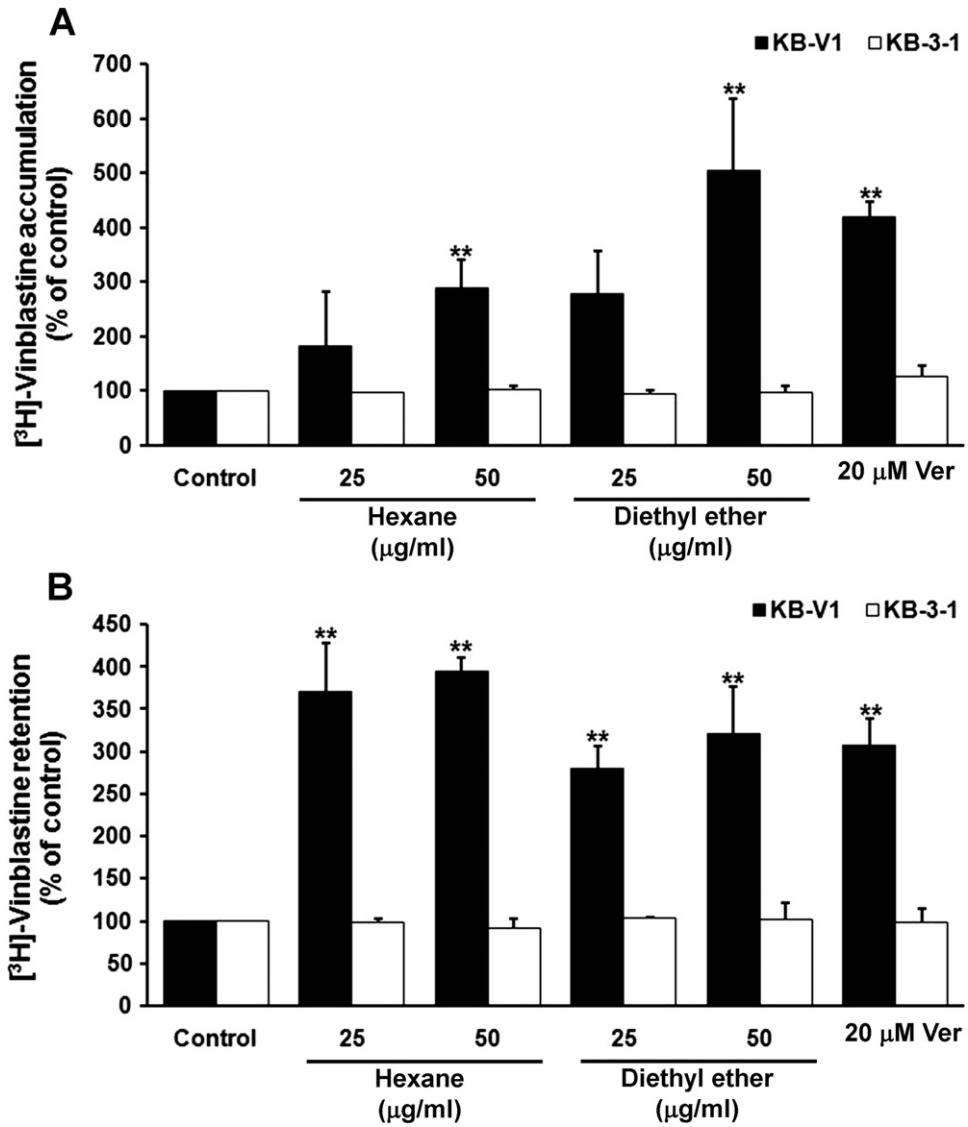

Fig. 1. The effect of BMLE on [^{3}H]-vinblastine accumulation (A) and retention (B) in KB-V1 and KB-3-1 cell lines. The amount of intracellular radioactivity in the presence of Ver and various concentrations of BMLE were examined as described in Materials and methods. The *Y*-axis shows the percentage of [^{3}H]-vinblastine accumulation, and the *X*-axis shows varying concentrations of BMLE. The mean value from three independent experiments is shown, and error bars indicate standard deviations. *P<.05; **P<.01, vs. vehicle control.

3.2. Structure identification of kuguacin J, an active component form BMLE

Kuguacin J (Fig. 2A) was obtained as an amorphous powder. The EIMS spectrum exhibited a $[M^+]$ ion peak at *m/z* 454 corresponding to the molecular formula $C_{30}H_{46}O_3$. Its IR spectrum displayed aldehyde carbonyl absorption at 1709/cm. In addition, the strong absorption band at 3464/cm revealed O–H stretching. The fragmentation ions in the mass spectrum at *m/z* 454 (M^+, 7), 442(9), 425 (68), 414(10), 396 (23), 323(100), 175(48), 135(75), 121(81) and 55(30) were also useful to obtain the structure of kuguacin J [18]. The ions at *m/z* 109 resulted from the olefinic side chain in the structure. Furthermore, independent evidence that the angular aldehyde group is readily eliminated from triterpenes was provided by the EIMS spectrum, which exhibited an intense M-29 peak (425). The high-resolution nuclear magnetic resonance ^{1}H and ^{13}C-NMR (1D and 2D) spectra were recorded at 400 MHz and 150 MHz, respectively, using a DPX on a BrÜker DPX 400 spectrometer in deuterochloroform as internal standard. The ^{1}H-NMR spectrum of kuguacin J exhibited characteristic proton signals of the aldehyde group, a downfield singlet at δ 9.75 and a broad singlet due to exomethylene protons at δ 4.85. The doublet at δ 6.13 (*J*=14.7) showed the geometry trans with proton at δ 5.61 (H-23). The ^{13}C-NMR spectrum data of δ_C 208.7, the most downfield signal, confirmed the presence of the carbonyl of the aldehyde group. In order to obtain more information about the location of the aldehyde group and double bonds in the structure of kuguacin J, a 2D-NMR HMBC and DQF-COSY were carried out. Furthermore, the purity of this compound was confirmed by the HRESIMS technique and exhibited *m/z*: 477.3339 $[M+Na]^+$ (calc. for $C_{30}H_{46}O_3Na$, 477.3344). Finally, this compound was identified as the previously known triterpenoid kuguacin J by comparing its physical and HPLC, IR, MS and NMR data with those reported in the literature [18–21].

Kuguacin J:, m.p. 165.7–166.8°C. (Lit[22] m.p. 166–169 °C). ^{13}C-NMR 150 MHz,$CDCl_3$: δ 20.57 (C-1), 29.94 (C-2), 76.28 (C-3), 42.30 (C-4), 145.42 (C-5), 125.09 (C-6), 76.13 (C-7), 47.51 (C-8), 50.74 (C-9), 40.54 (C-10), 23.11 (C-11), 29.86 (C-12), 45.40 (C-13), 48.48 (C-14), 33.46 (C-15), 28.19 (C-16), 49.60 (C-17), 14.69 (C-18), 207.86 (C-19), 38.1 (C-20), 19.65 (C-21), 39.67 (C-22), 138.8 (C-23), 134.27 (C-24), 142.13 (C-25),114.14 (C-26), 19.40 (C-27), 27.09 (C-28), 27.69 (C-29). ^{1}H-NMR 400 MHz,$CDCl_3$: δ 1.24 (H-1), 1.31 (H-2), 3.55 (H-3), 5.6 (H-6), 3.41 (H-7), 2.09 (H-8), 2.5 (H-10), 1.63 (H-11), 1.31 (H-12), 1.4 (H-15), 1.31 (H-16), 1.49 (H-17), 0.91 (H-18), 9.75 (H-19), 1.53 (H-20), 0.89 (H-21), 2.25 (H-22), 5.61 (H-23), 6.13 (H-24), 4.85 (H-26), 1.84 (H-27), 1.06 (H-28), 1.39 (H-29).

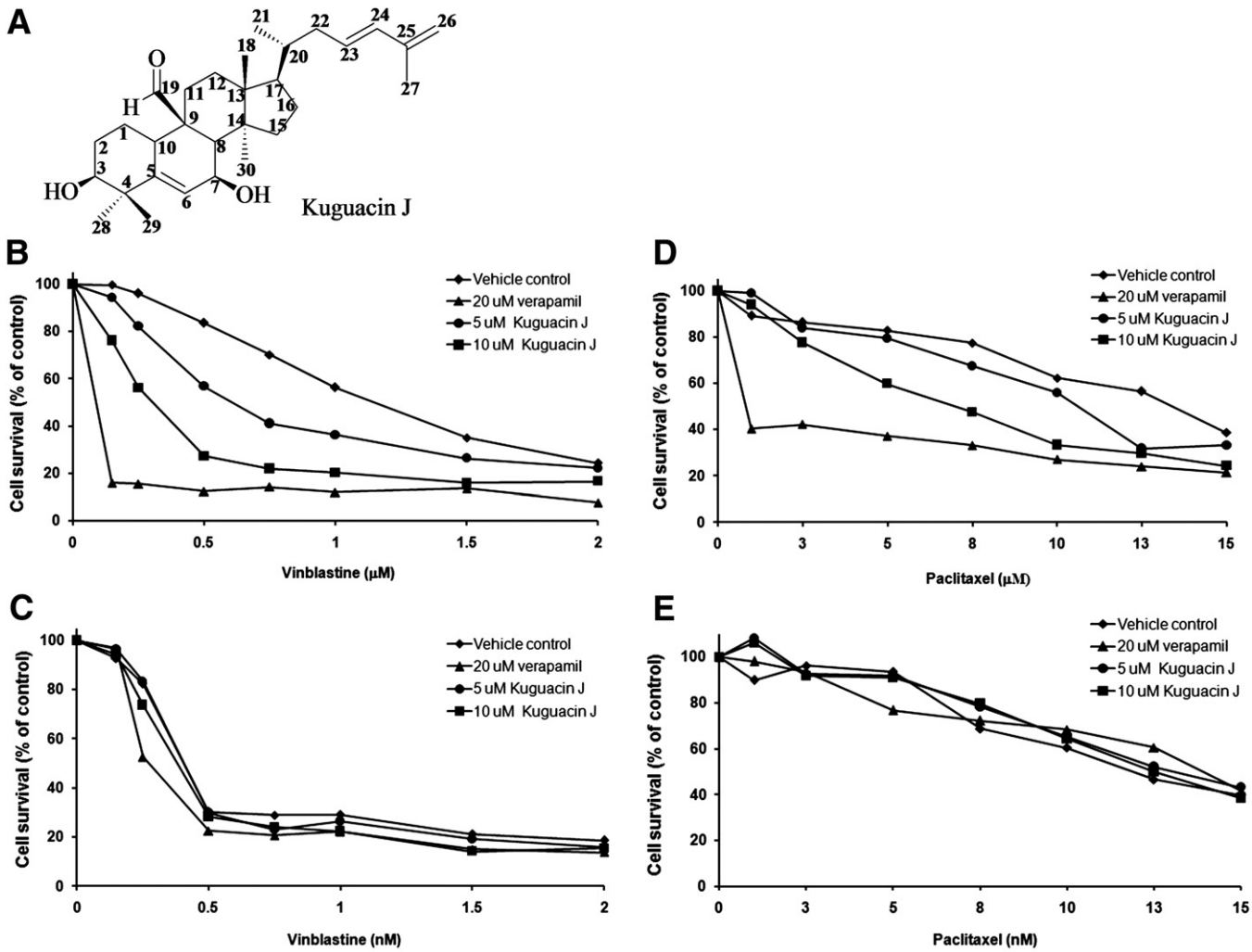

Fig. 2. Structure of kuguacin J (A) and the effect of kuguacin J on vinblastine and paclitaxel cytotoxicity in KB-V1 (B, D) and KB-3-1 (C, E) cell lines. Cells were incubated in the presence or absence of kuguacin J in combination with vinblastine or paclitaxel. The number of viable cells was determined by an MTT assay. The *Y*-axis shows the percentage of cell survival, and the *X*-axis shows varying concentrations of kuguacin J. Each point represents the mean of three independent experiments performed in triplicate.

Table 2
Modulation of resistance to vinblastine and paclitaxel in KB cells by kuguacin J

	IC_{50}[a]	Relative resistance[b]
Vinblastine treatment		
KB-3-1	0.4±0.12 nM	1
KB-V1	1.3±0.28 μM	3023
Kuguacin J		
KB-V1+5 μM kuguacin J	0.7±0.38 μM	1595*
KB-V1+10 μM kuguacin J	0.3±0.03 μM	700**
KB-V1+20 μM verapamil	0.1±0.04 μM	464**
Paclitaxel treatment		
KB-3-1	7.3±0.16 nM	1
KB-V1	13.3±1.16 μM	1821
Kuguacin J		
KB-V1+5 μM kuguacin J	8.3±0.58 μM	950*
KB-V1+10 μM kuguacin J	5.2±0.29 μM	579**
KB-V1+20 μM verapamil	4.5±0.50 μM	545**

*P<.05; **P<.01, vs. control treated without kuguacin J.
[a] Determined by the MTT assay, and the values are means±S.D. of three independent experiments.
[b] IC_{50} of KB-V1/IC50 of KB-3-1. Each point represents the mean (±S.D.) of three independent experiments performed in triplicate.

3.3. Effect of kuguacin J on cytotoxicity of paclitaxel and vinblastine in KB-3-1 and KB-V1 cells

To examine the MDR-reversing property of kuguacin J on paclitaxel and vinblastine cytotoxicity, the growth inhibition of cells was investigated in response to increasing concentrations of paclitaxel or vinblastine with or without kuguacin J. The results showed that 5 and 10 μM of kuguacin J increased sensitivity of KB-V1 cells to both vinblastine and paclitaxel, 1.9- and 4.3-fold, respectively, for vinblastine, and 1.9- and 3.2-fold, respectively, for paclitaxel, while similar treatment of KB-3-1 cells provided no modulating effect (Table 2, Fig. 2B–E).

3.4. Effect of kuguacin J on C-AM and Rh123 accumulation

We next studied the effect of kuguacin J on P-gp function. Accumulation of fluorescent substrates of P-gp (C-AM and Rh123) was determined using flow cytometry. These fluorescent substrates were chosen to determine whether the inhibitory effects of kuguacin J are substrate specific or not. The results demonstrated the accumulation of C-AM was increased by 2.2-, 2.9-, 3.5- and 4.1-fold when KB-V1 cells were treated with 10, 20, 40 and 60 μM of kuguacin J, respectively (Fig. 3A). The same treatment of kuguacin J showed that the accumulation of Rh123 was also significantly increased by 2.5-, 2.8-, 3.1- and 3.5-fold, respectively (Fig. 3B). These effects were not found in wild-type KB-3-1 cells (Fig. 3A, B).

3.5. Effect of kuguacin J on [^{3}H]-vinblastine accumulation and efflux

To confirm the P-gp-function inhibitory effect of kuguacin J, drug accumulation and efflux assays were performed. It was found that kuguacin J at 10, 20 and 40 μM increased [^{3}H]-vinblastine

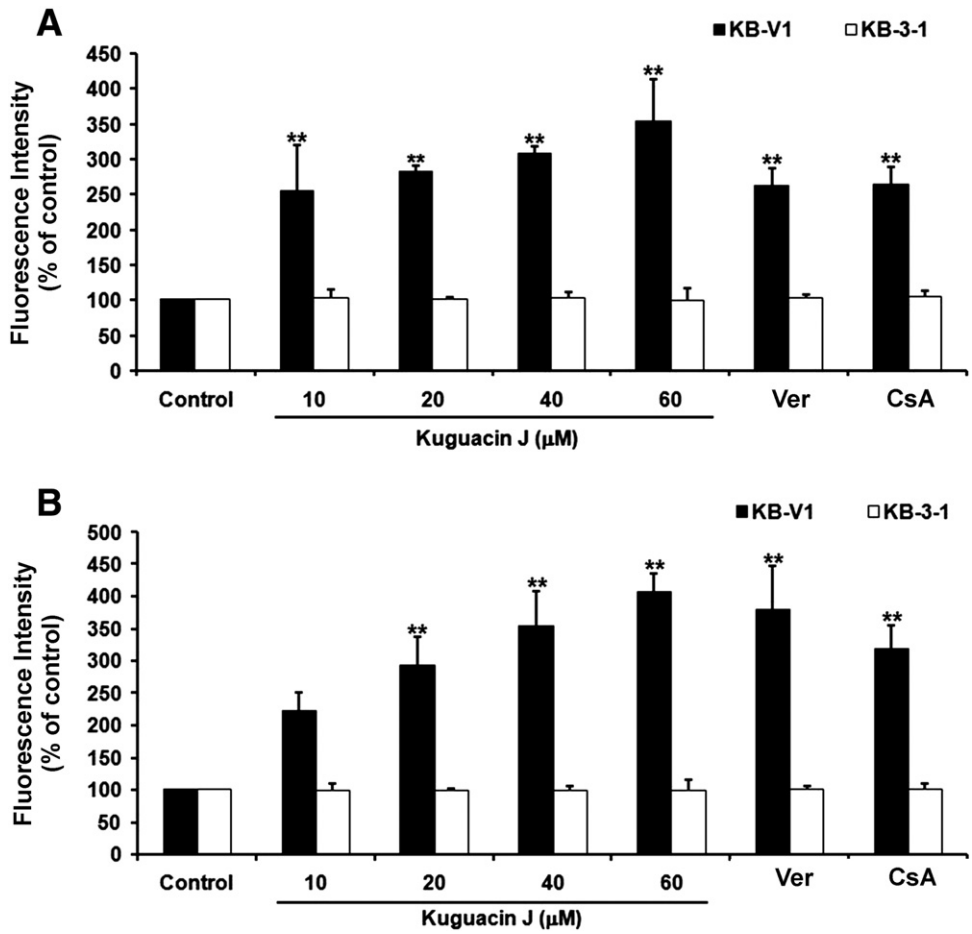

Fig. 3. Effect of kuguacin J on C-AM (A) and Rh123 (B) accumulation in KB-V1 and KB-3-1 cell lines. The fluorescence intensity in the presence of CsA, Ver and various concentrations of kuguacin J were analyzed using FACScan as described in Materials and methods. The *Y*-axis shows the percentage of the accumulation of fluorescent substrates, and the *X*-axis shows varying concentrations of kuguacin J. The mean value from three independent experiments is shown, and error bars indicate standard deviations. *P<.05; **P<.01, vs. vehicle control.

accumulation in KB-V1 cells by about 1.4-, 2.3- and 4.5-fold, respectively (Fig. 4A). Accumulation of [^{3}H]-vinblastine in drug-sensitive KB-3-1 cells treated with kuguacin J, Ver or CsA did not differ from its accumulation in cells without any treatment (Fig. 4A).

The effect of kuguacin J on the P-gp-mediated efflux of vinblastine showed that kuguacin J at concentrations 10, 20 and 40 μM caused a dose-dependent decrease in the amount of [^{3}H]-vinblastine efflux from KB-V1 cells and resulted in an increase in intracellular [^{3}H]-vinblastine retention by approximately 3.5-, 5.2- and 6.5-fold, respectively (Fig. 4B). These effects were not observed in KB-3-1 cells (Fig. 4B).

3.6. Effect of kuguacin J on photoaffinity labeling of P-gp with [^{125}I]-IAAP

To study the interaction of kuguacin J with the substrate-binding sites of P-gp, we monitored the effect of kuguacin J on the crosslinking of [^{125}I]-IAAP with P-gp, which is a transport substrate of P-gp [23]. This photoaffinity labeling with transport substrate is a useful tool to investigate the interaction of the drugs at the substrate-binding sites of P-gp. Fig. 5 clearly shows that kuguacin J inhibits the photo-crosslinking of P-gp with [^{125}I]-IAAP with an IC_{50} of 8.3±5.4 μM (Fig. 5). This suggests that kuguacin J interacts directly with the substrate-binding site of P-gp.

3.7. Effect of kuguacin J on ATPase activity of P-gp

An ATPase assay was carried out to determine whether kuguacin J, by interacting at the transport-substrate site, influences ATPase activity of P-gp since this pump utilizes the energy of ATP to transport a substrate from inside to outside the cell, and transport substrates often stimulate P-gp-mediated ATP hydrolysis. As shown in Fig. 6, kuguacin J had no effect on the ATP hydrolysis except that a lower concentration of kuguacin J (50–100 nM) produced a 1.1- to 1.3-fold stimulation of ATP hydrolysis (17.8–20.9 nmol P_i/mg protein/min) compared with basal activity (15.7 nmol P_i/mg protein/min; Fig. 6). To further characterize the nature of kuguacin J interaction, we investigated the effect of kuguacin J on verapamil-stimulated ATPase activity. As shown in Fig. 7A, kuguacin J inhibited verapamil-stimulated ATPase activity in a dose-dependent manner. The same data were transformed to the linear form of $1/V$ versus $1/S$ (Lineweaver–Burke plot) (Fig. 7B) to analyze the type of inhibition (i.e., competitive or noncompetitive). Fig. 7B clearly showed that

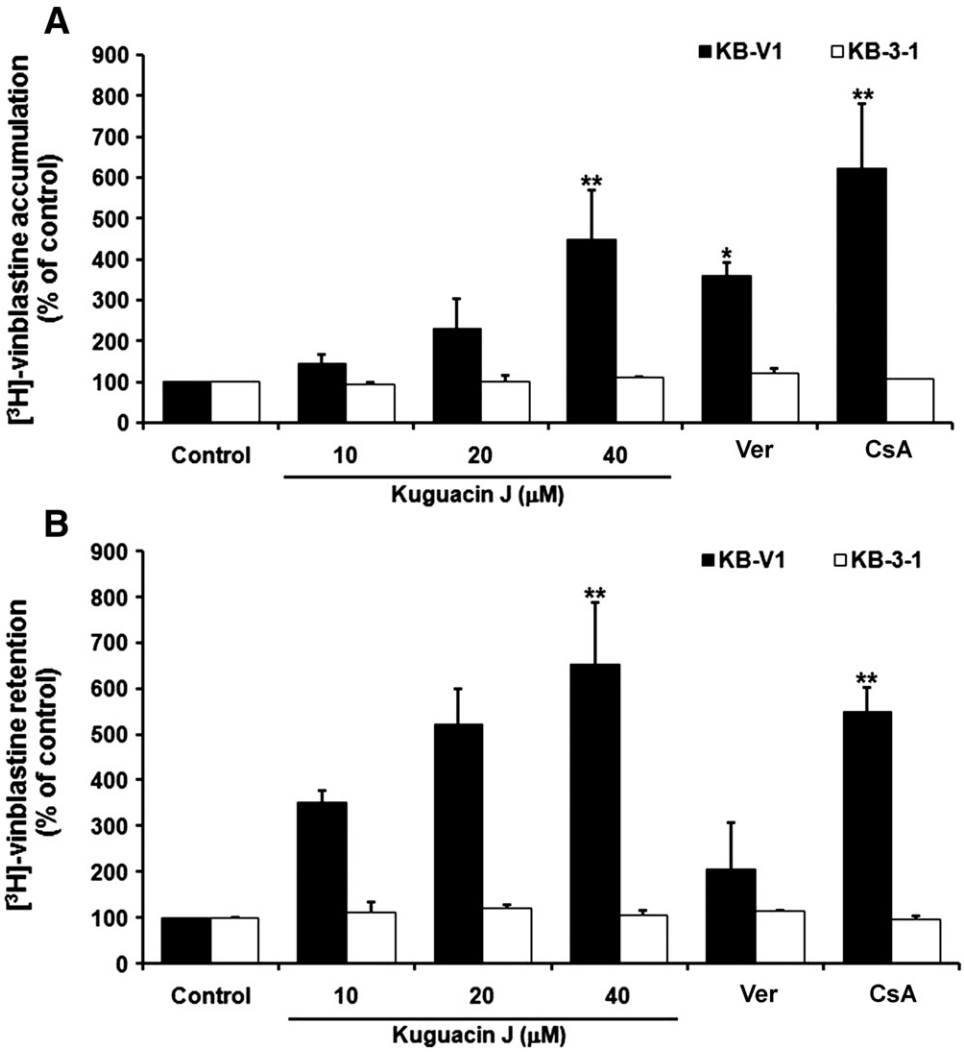

Fig. 4. Effect of kuguacin J on [^{3}H]-vinblastine accumulation (A) and efflux (B) in KB-V1 and KB-3-1 cell lines. The amount of intracellular radioactivity in the presence of CsA, Ver and various concentrations of the kuguacin J was determined as described in Materials and methods. The *Y*-axis shows the percentage of [^{3}H]-vinblastine accumulation, and the *X*-axis shows varying concentrations of kuguacin J. The mean value from three independent experiments is shown, and error bars indicate standard deviations. *P<.05; **P<.01, vs. vehicle control.

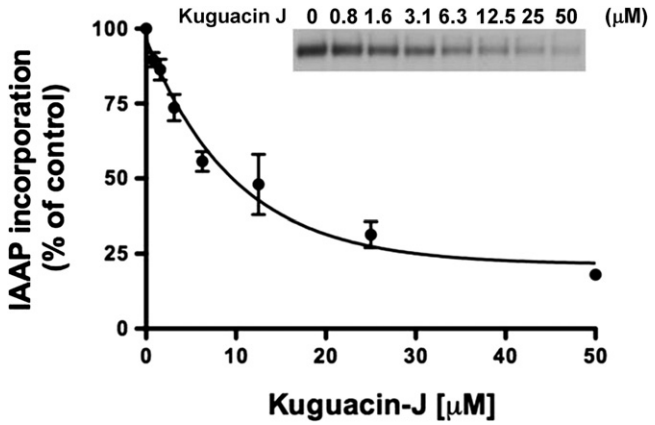

Fig. 5. Effect of kuguacin J on the incorporation of the photoaffinity substrate, [^{125}I]-IAAP, into P-gp. The photolabeling of P-gp with [^{125}I]-IAAP to P-gp was monitored as described in Materials and methods in the presence of increasing concentrations of kuguacin J (0–50 μM). The *Y*-axis shows the percentage of [^{125}I-IAAP incorporation, and the *X*-axis shows varying concentrations of kuguacin J. The mean value from three independent experiments is shown, and error bars indicate standard deviations. The IC_{50} value for the inhibition of [^{125}I-IAAP incorporation into P-gp was 8.3±5.4 μM. The autoradiogram from a representative experiment from three independent experiments is shown.

kuguacin J acts as competitive inhibitor of verapamil-stimulated ATPase activity. From these plots, the apparent K_i of kuguacin J was determined to be 2.4±1.1 μM (n =3).

4. Discussion

Resistance to chemotherapy is a major problem in the management of cancer patients and is caused by various molecular mechanisms. One of these mechanisms is the overexpression of MDR1/P-gp, which is the major cause of MDR of human cancers. Potent MDR modulators are being investigated in clinical trials. Verapamil, a calcium channel blocker, and cyclosporin A, an immunosuppressive agent, are the most effective P-gp inhibitors in

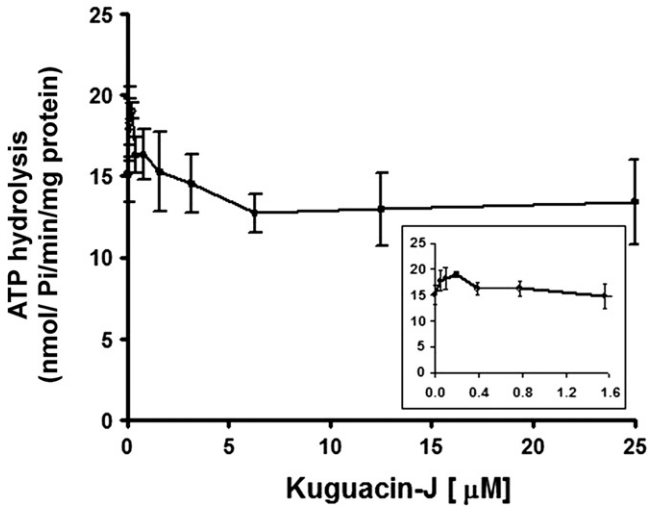

Fig. 6. Effect of kuguacin J on ATP hydrolysis by P-gp. The vanadate-sensitive ATPase activity of P-gp was determined by using the P_i release assay, as described in Materials and methods, in the presence of increasing concentrations of kuguacin J (0–25 μM). The *Y*-axis shows the ATP hydrolysis (nmol P_i/mg protein/min), and *X*-axis shows varying concentrations of kuguacin J. The mean value from three independent experiments is shown, and error bars indicate standard deviations. The inset shows ATPase activity in the presence of low concentrations of kuguacin J (0–1.6 μM).

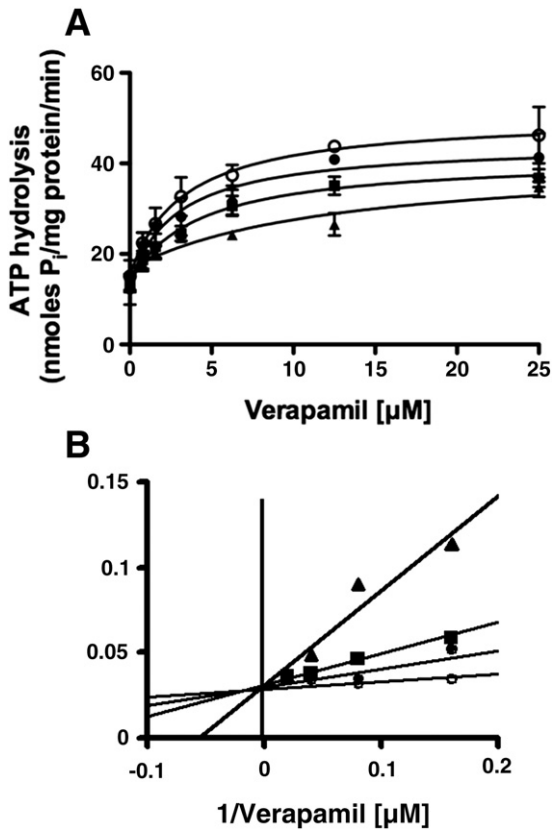

Fig. 7. Effect of kuguacin J on verapamil-stimulated ATP hydrolysis. (A) The kinetics of inhibition of the verapamil-stimulated ATPase activity by kuguacin J. The vanadate-sensitive ATPase activity of P-gp was determined by using the P_i release assay, as described in Materials and methods, in the presence of increasing concentration of verapamil (0–25 μM) at four different concentrations of kuguacin J (0, 2.5, 5 and 10 μM). The curve was fitted to the Michaelis–Menten equation: $V=V_0+(V_{max}-V_0)S/(S+K_m)$. The *Y*-axis shows the ATP hydrolysis (nmol P_i/mg protein/min), and *X*-axis shows varying concentrations of verapamil. The mean value from three independent experiments is shown, and error bars indicate standard deviations. (B) The Lineweaver–Burke plot (1/ATP hydrolysis vs. 1/verapamil) of the data in (A). The apparent K_i (2.4±1.1 μM; n =3) is obtained from $1/V=1/V_{max}+K_m/V_{max}(1+I/K_i)(1/S)$ equation as described [24].

vitro, but they have limited clinical use. Many current studies are focused on dietary herbs due to the fact that these have been used for centuries without producing any harmful side effects [2,14,25–28].

Bitter melon (*M. charantia*) is a plant that grows in tropical areas of Asia, the Caribbean and South America and has a long history of use as a folk medicine. It has been reported that bitter melon has antidiabetic, antiviral, antioxidative and antineoplastic effects [29]. Some functional components have already been identified such as vegetable insulin and charantin, having hypoglycemic effects [30], and MAP30, a 30-kDa protein from the seeds and fruits of bitter melon, having antiviral effects [10,31]. In a previous study, we reported that BMLE was able to reverse the MDR phenotype [12] and to inhibit rat prostate cancer invasion and migration in vitro and decrease lung metastasis in vivo [28]. However, the active compound (s) still remains to be identified. In this study, bioguided fractionation was used to identify the active component(s) in BMLE which acts to modulate the function of P-gp and the MDR phenotype in multidrug-resistant human cervical carcinoma. The ethanolic fraction was subsequently extracted with solvents increasing in polarity (i.e., ethanol, hexane, diethyl ether, chloroform and ethyl acetate). These extraction samples were tested for their abilities to modulate the function of P-gp in the multidrug-resistant human cervical carcinoma KB-V1 cells (with overexpression of P-gp) in comparison with

wild-type drug-sensitive KB-3-1 cells (with low expression of P-gp). Among the extracts tested, the hexane and diethyl ether fractions had the most effective MDR-reversing properties (Table 1), increased intracellular [3H]-vinblastine accumulation and decreased the [3H]-vinblastine efflux in KB-V1 cells, while no change was observed in KB-3-1 cells (data not shown). As the percentage yield of diethyl ether fraction was higher than hexane fraction, we therefore purified the active component using the diethyl ether fraction as a staring material (Materials and methods). Bioassay-guided fractionation led us to isolate a purified white crystal. The IR, NMR and MS data of the compound were compared with previous reports [18], and it was identified as kuguacin J (3,7,23-trihydroxycucurbita-5,24-dien-19-al) (Fig. 2A).

We further examined the MDR-reversing property of kuguacin J on the cytotoxicity of vinblastine or paclitaxel in KB-V1 and KB-3-1 cells and found that kuguacin J increased the sensitivity of KB-V1 cells to vinblastine and paclitaxel, but did not have this effect on KB-3-1 cells (Table 2, Fig. 2B–D). Moreover, treatment of KB-V1 and KB-3-1 cells with kuguacin J yielded a marked increase in C-AM and Rh123 accumulations in a concentration-dependent manner in KB-V1 cells but had no effect on KB-3-1 cells. C-AM and Rh123 are known to be good substrates for P-gp, indicating that kuguacin J modulates intracellular drug levels by inhibiting P-gp activity. We also confirmed the inhibitory effect of kuguacin J on P-gp function by [^{3}H]-vinblastine transportation assays. It was found that kuguacin J also increased [3H]-vinblastine accumulation in KB-V1 cells and decreased [3H]-vinblastine efflux from KB-V1 cells. A previous study showed that P-gp expression in KB-V1 cells was not affected by treating the cells with BMLE [12]. Taken together, the data suggest that kuguacin J inhibits P-gp activity but not its expression.

The photoaffinity labeled transport substrate of P-gp, [^{125}I]-IAAP, has been used extensively to study the interaction of the modulators at the substrate-binding site of P-gp [23]. It is also known that P-gp can be specifically labeled with [^{125}I]-IAAP, and drug substrates of P-gp inhibit the photo-crosslinking of [^{125}I]-IAAP to P-gp [16]. As shown in Fig. 5, kuguacin J inhibited the photo-crosslinking of [^{125}I]-IAAP to P-gp in a concentration-dependent manner. This is direct evidence that kuguacin J interacts with the substrate-binding site of P-gp. To further verify the interaction of kuguacin J with P-gp, an ATPase assay was employed, which is another useful assay to study the interaction of transport substrates with P-gp, as ATP hydrolysis is coupled to the transport function of this transporter [17]. Although kuguacin J had a negligible effect on the basal ATPase activity of P-gp, a low concentration of kuguacin J (50–100 nM) slightly stimulated P-gp-mediated ATP hydrolysis (Fig. 6). This finding also implies that kuguacin J interacts with the substrate-binding site of P-gp.

The published reports on P-gp drug-binding data and kinetic results have suggested the existence of multiple overlapping substrate-binding sites within the P-gp [32,33]. This means that the substrates for P-gp may interact competitively as well as noncompetitively (allosterically) for binding to this protein. To further characterize the nature of interaction of kuguacin J, we investigated the effect of kuguacin J on verapamil-stimulated ATPase activity. Previous studies have shown that verapamil stimulates P-gp-mediated ATP hydrolysis approximately three- to fourfold [34,35]. However, when P-gp is treated with verapamil and other drug substrates, a concentration-dependent inhibition of verapamil-stimulated ATPase activity is observed [36]. It has been postulated that this inhibition is a consequence of competition at and displacement of verapamil at the substrate-binding site of P-gp [36]. In Fig. 7A, kuguacin J indeed inhibited the verapamil-stimulated ATPase activity of P-gp. Furthermore, the kinetic analyses clearly showed that kuguacin J competes with verapamil for the substrate-binding site of P-gp (Fig. 7B). Taken together, these biochemical data suggest that kuguacin J inhibits the transport function of P-gp by interacting with the substrate-binding site of P-gp where verapamil also binds.

In conclusion, this study is the first to demonstrate that kuguacin J, a compound isolated from BMLE, is an effective inhibitor of P-gp activity and could be a candidate molecule for treating cancers exhibiting P-gp-mediated MDR. The results reported here open the possibility for investigations of the effect of kuguacin J in animal experiments to determine if this compound has potential as an effective chemosensitizer to be used in combination with conventional chemotherapy.

Acknowledgments

This work was supported by the National Research Council of Thailand, the Royal Golden Jubilee Scholarship Ph.D. Program (R.G.J.) and the Intramural Research Program of the National Institutes of Health, National Cancer Institute, Center for Cancer Research (S.O. and S.V.A.). We thank George Leiman for editorial assistance in preparation of the manuscript.

References

[1] Tan B, Piwnica-Worms D, Ratner L. Multidrug resistance transporters and modulation. Curr Opin Oncol 2000;12:450–8.
[2] Anuchapreeda S, Leechanachai P, Smith MM, Ambudkar SV, Limtrakul PN. Modulation of P-glycoprotein expression and function by curcumin in multidrug-resistant human KB cells. Biochem Pharmacol 2002;64:573–82.
[3] Larsen AK, Escargueil AE, Skladanowski A. Resistance mechanisms associated with altered intracellular distribution of anticancer agents. Pharmacol Ther 2000;85:217–29.
[4] Lehnert M. Chemotherapy resistance in breast cancer. Anticancer Res 1998:18.
[5] Schoenlein PV, Shen DW, Barrett JT, Pastan I, Gottesman MM. Double minute chromosomes carrying the human multidrug resistance 1 and 2 genes are generated from the dimerization of submicroscopic circular DNAs in colchicine-selected KB carcinoma cells. Mol Biol Cell 1992;3:507–20.
[6] Varma MV, Ashokraj Y, Dey CS, Panchagnula R. P-glycoprotein inhibitors and their screening: a perspective from bioavailability enhancement. Pharmacol Res 2003;48:347–59.
[7] Nagasawa H, Watanabe K, Inatomi H. Effects of bitter melon (*Momordica charantia* l.) or ginger rhizome (*Zingiber offifinale rosc*) on spontaneous mammary tumorigenesis in SHN mice. Am J Chin Med 2002;30:195–205.
[8] Deep G, Dasgupta T, Rao AR, Kale RK. Cancer preventive potential of *Momordica charantia* L. against benzo(a)pyrene induced fore-stomach tumourigenesis in murine model system. Indian J Exp Biol 2004;42:319–22.
[9] Shi H, Hiramatsu M, Komatsu M, Kayama T. Antioxidant property of Fructus Momordicae extract. Biochem Mol Biol Int 1996;40:1111–21.
[10] Lee-Huang S, Huang PL, Chen HC, Bourinbaiar A, Huang HI, Kung HF. Anti-HIV and anti-tumor activities of recombinant MAP30 from bitter melon. Gene 1995;161:151–6.
[11] Cunnick JE, Sakamoto K, Chapes SK, Fortner GW, Takemoto DJ. Induction of tumor cytotoxic immune cells using a protein from the bitter melon (*Momordica charantia*). Cell Immunol 1990;126:278–89.
[12] Limtrakul P, Khantamat O, Pintha K. Inhibition of P-glycoprotein activity and reversal of cancer multidrug resistance by *Momordica charantia* extract. Cancer Chemother Pharmacol 2004;54:525–30.
[13] Legrand O, Simonin G, Perrot JY, Zittoun R, Marie JP. Pgp and MRP activities using calcein-AM are prognostic factors in adult acute myeloid leukemia patients. Blood 1998;91:4480–8.
[14] Limtrakul P, Chearwae W, Shukla S, Phisalphong C, Ambudkar SV. Modulation of function of three ABC drug transporters, P-glycoprotein (ABCB1), mitoxantrone resistance protein (ABCG2) and multidrug resistance protein 1 (ABCC1) by tetrahydrocurcumin, a major metabolite of curcumin. Mol Cell Biochem 2007;296:85–95.
[15] Ramachandra M, Ambudkar SV, Chen D, Hrycyna CA, Dey S, Gottesman MM, et al. Human P-glycoprotein exhibits reduced affinity for substrates during a catalytic transition state. Biochemistry 1998;37:5010–9.
[16] Sauna ZE, Ambudkar SV. Evidence for a requirement for ATP hydrolysis at two distinct steps during a single turnover of the catalytic cycle of human P-glycoprotein. Proc Natl Acad Sci U S A 2000;97:2515–20.
[17] Ambudkar SV. Drug-stimulatable ATPase activity in crude membranes of human MDR1-transfected mammalian cells. Methods Enzymol 1998;292:504–14.
[18] Chen JC, Liu WQ, Lu L, Qiu MH, Zheng YT, Yang LM, et al. Kuguacins F-S, cucurbitane triterpenoids from *Momordica charantia*. Phytochemistry 2009;70:133–40.

[19] Chen J, Tian R, Qiu M, Lu L, Zheng Y, Zhang Z. Trinorcucurbitane and cucurbitane triterpenoids from the roots of *Momordica charantia*. Phytochemistry 2008;69: 1043–8.
[20] Mekuria DB, Kashiwagi T, Tebayashi S, Kim CS. Cucurbitane triterpenoid oviposition deterrent from *Momordica charantia* to the leafminer, *Liriomyza trifolii*. Biosci Biotechnol Biochem 2005;69:1706–10.
[21] Puspawati N. Isolation and identification momordicin I from leaves extract of *Momordica charantia* L. J Kimia 2008;2:53–6.
[22] Choi SZ, Yang MC, Choi SU, Lee KR. Cytotoxic terpenes and lignans from the roots of *Ainsliaea acerifolia*. Arch Pharm Res 2006;29:203–8.
[23] Maki N, Hafkemeyer P, Dey S. Allosteric modulation of human P-glycoprotein. Inhibition of transport by preventing substrate translocation and dissociation. J Biol Chem 2003;278:18132–9.
[24] Litman T, Zeuthen T, Skovsgaard T, Stein WD. Competitive, non-competitive and cooperative interactions between substrates of P-glycoprotein as measured by its ATPase activity. Biochim Biophys Acta Mol Basis Dis 1997;1361:169–76.
[25] Chearwae W, Anuchapreeda S, Nandigama K, Ambudkar SV, Limtrakul P. Biochemical mechanism of modulation of human P-glycoprotein (ABCB1) by curcumin I, II, and III purified from turmeric powder. Biochem Pharmacol 2004;68:2043–52.
[26] Limtrakul P, Khantamat O, Pintha K. Inhibition of P-glycoprotein function and expression by kaempferol and quercetin. J Chemother 2005;17:86–95.
[27] Limtrakul P, Siwanon S, Yodkeeree S, Duangrat C. Effect of *Stemona curtisii* root extract on P-glycoprotein and MRP-1 function in multidrug-resistant cancer cells. Phytomedicine 2007;14:381–9.
[28] Pitchakarn P, Ogawa K, Suzuki S, Takahashi S, Asamoto M, Chewonarin T, et al. *Momordica charantia* leaf extract suppresses rat prostate cancer progression in vitro and in vivo. Cancer Sci 2010;101:2234–40.
[29] Basch E, Gabardi S, Ulbricht C. Bitter melon (*Momordica charantia*): a review of efficacy and safety. Am J Health Syst Pharm 2003;60:356–9.
[30] Miura T, Itoh C, Iwamoto N, Kato M, Kawai M, Park SR, et al. Hypoglycemic activity of the fruit of the *Momordica charantia* in type 2 diabetic mice. J Nutr Sci Vitaminol (Tokyo) 2001;47:340–4.
[31] Lee-Huang S, Huang PL, Nara PL, Chen HC, Kung HF, Huang P, et al. MAP 30: a new inhibitor of HIV-1 infection and replication. FEBS Lett 1990;272: 12–8.
[32] Safa AR. Photoaffinity labels for characterizing drug interaction sites of P-glycoprotein. Methods Enzymol 1998;292:289–307.
[33] Ambudkar SV, Kim IW, Sauna ZE. The power of the pump: mechanisms of action of P-glycoprotein (ABCB1). Eur J Pharm Sci 2006;27:392–400.
[34] Sarkadi B, Price EM, Boucher RC, Germann UA, Scarborough GA. Expression of the human multidrug resistance cDNA in insect cells generates a high activity drug-stimulated membrane ATPase. J Biol Chem 1992;267:4854–8.
[35] Ambudkar SV, Lelong IH, Zhang J, Cardarelli CO, Gottesman MM, Pastan I. Partial purification and reconstitution of the human multidrug-resistance pump: characterization of the drug-stimulatable ATP hydrolysis. Proc Natl Acad Sci U S A 1992;89:8472–6.
[36] Rao US, Scarborough GA. Direct demonstration of high affinity interactions of immunosuppressant drugs with the drug binding site of the human P-glycoprotein. Mol Pharmacol 1994;45:773–6.